ERK Modulates DNA Bending and Enhancesome Structure by Phosphorylating HMG1-Boxes 1 and 2 of the RNA Polymerase I Transcription Factor UBF†

Victor Y. Stefanovsky,‡ Frédèric Langlois,‡ David Bazett-Jones,§ Guillaume Pelletier,‡ and Tom Moss*,‡

Cancer Research Centre and Department of Medical Biology of Laval University, Centre de Recherche de l'Hôtel-Dieu de Québec, 9 rue McMahon G1R 2J6 Québec, QC, Canada, and Department of Biochemistry, University of Toronto and Program in Cell Biology, Hospital for Sick Children, 555 University Avenue, Toronto, ON M5G 1X8, Canada

Received September 4, 2005; Revised Manuscript Received January 11, 2006

ABSTRACT: Transcription of the ribosomal RNA genes of mammals by RNA polymerase I is rapidly activated by epidermal growth factor via the MAP-kinase (ERK) signaling cascade. This activation is mediated by direct phosphorylation of the HMG box DNA binding domains of the architectural transcription factor UBF. Mutation of the ERK sites of UBF inhibits its normal function and blocks growth factor activation of ribosomal transcription. UBF has little or no DNA sequence selectivity and binds throughout the ribosomal genes, defining a specialized chromatin. Indeed, the HMG boxes of UBF induce looping of the ribosomal DNA to create the *enhancesome*, a structure somewhat reminiscent of the nucleosome. Here, we show that both ERK phosphorylation and mutations that simulate this phosphorylation decrease the affinity of the individual HMG boxes of UBF for linear ribosomal DNA but have little or no effect on the capacity of these HMG boxes to bind to pre-bent DNA and do not affect the overall binding constant of UBF for the DNA. Electron spectroscopic imaging showed that ERK site UBF mutants do not induce the characteristic DNA looping of the *enhancesome* and associate with no more than half of the *enhancesomal* DNA. The data demonstrate that ERK phosphorylation of UBF prevents DNA bending by its first two HMG boxes, leading to a cooperative unfolding of the *enhancesome*.

Ribosome biogenesis is a necessary function but at the same time a major undertaking for all organisms. Expression of the highly repeated ribosomal RNA genes and the more than 200 ribosomal and accessory protein genes accounts for more than 50% of total nuclear transcription in proliferating mammalian cells. The 18S, 5.8S, and 28S ribosomal RNAs (rRNAs) are transcribed as a single 45S precursor by a specialized polymerase, RNA polymerase I (RPI). These rRNAs form the structural and catalytic scaffold of the ribosome, and as such, their production can only be regulated at the transcriptional level. Alone, transcription of the rRNA genes by RPI accounts for some 35% of all nuclear transcription activity. Until quite recently, it was assumed that the ribosomal RNA genes of mammals respond to changes in cell proliferation and growth rate, but do so in an indirect and sluggish way. This opinion was mainly based on cell starvation and hormone treatment of mammalian tissue culture, and the results seemed quite logical given that the ribosome typically has a half-life of three or more days (*1*). Recent work, however, has demonstrated that transcription of the ribosomal genes in mouse and human responds rapidly and directly to growth factor stimulation. Activation occurs within 10 to 15 min of cell stimulation and thus represents one of a limited number of so-called immediate gene responses (*2*). Conversely, withdrawal of growth stimuli was found to induce an immediate shutdown of human and mouse ribosomal RNA transcription (*2*). Given the length of the cell cycle, the reason such a rapid activation of ribosomal transcription should be necessary in mammalian cells is not quite clear. It is perhaps related to the role the nucleolus plays in the regulation of cell proliferation than to ribosome biogenesis per se (*3*−*7*). On the other hand, a rapid shutdown of rRNA transcription is analogous to the well-documented phenomenon in microorganisms referred to as the "stringent response" and could possibly play a similar protective role.

The "stringent" regulation of ribosomal RNA transcription in mammalian cells was shown to depend on a direct phosphorylation of the first two HMG box DNA binding domains of the transcription factor UBF by MAP-kinase (ERK1/2) (*2*), Figure 1B. A similar response, dependent on the phosphorylation status of Rrn3/TIF-IA, was later observed and was shown also to depend on activation of the ERK cascade (*8*). In the sequence of events leading to the assembly of a RPI preinitiation complex, UBF was originally believed to be the first factor to bind the ribosomal DNA where it was thought to enhance recruitment of the other basal factor SL1(TIF-IB) and the polymerase (*9*−*14*). However, more recent work has suggested that a role for UBF in preinitiation complex formation is doubtful (*15*). Further, UBF has little or no sequence preference and is

† This work was supported by an operating grant from the Canadian Institutes of Health Research and a FCAR-FRSQ Santé (Québec) scholarship to G.P.

* To whom correspondence should be addressed. E-mail: Tom.Moss@crhdq.ulaval.ca.

‡ Cancer Research Centre and Department of Medical Biology of Laval University.

§ University of Toronto and Hospital for Sick Children.

10.1021/bi051782h CCC: $33.50
Published on Web 02/24/2006

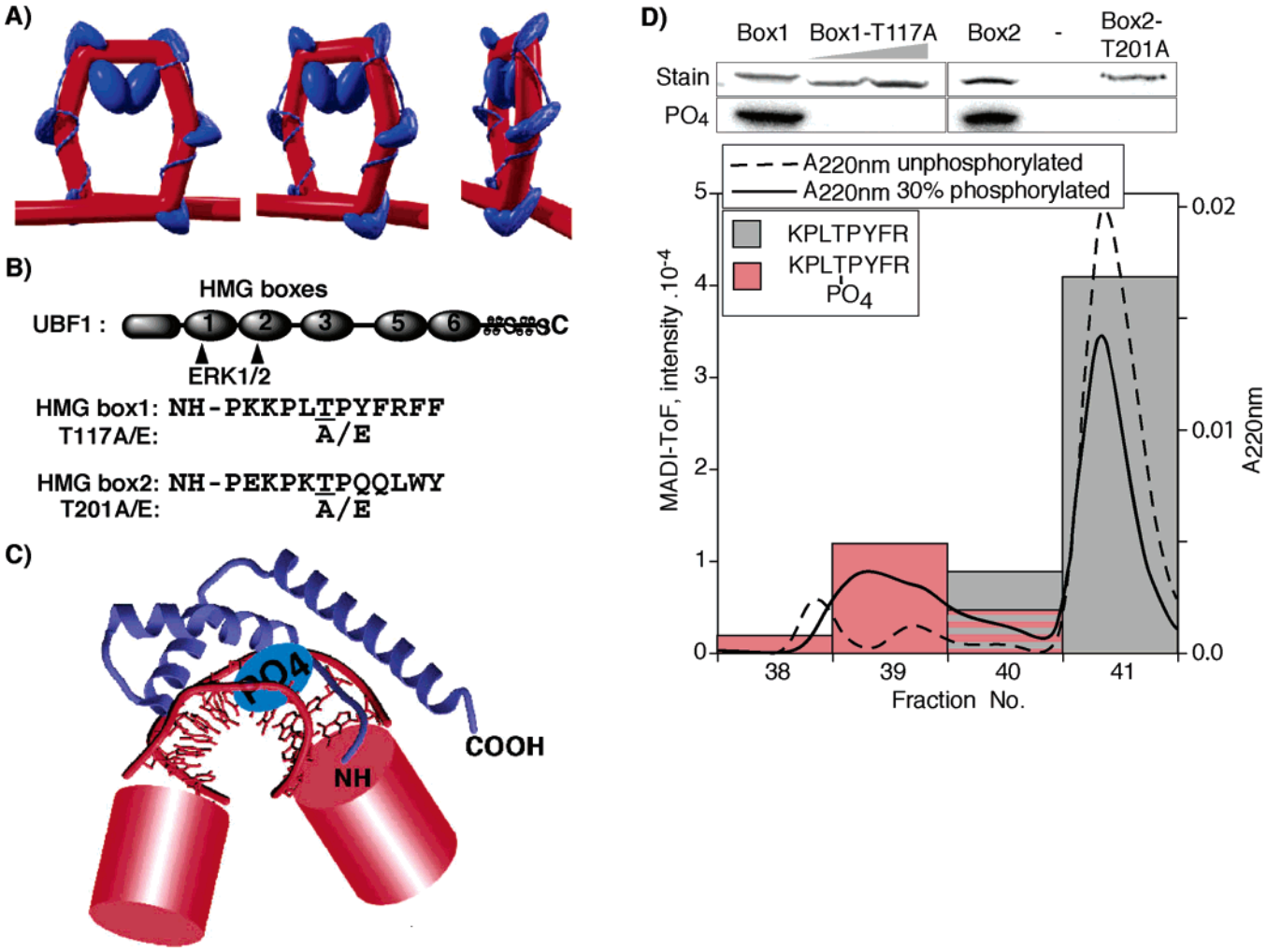

FIGURE 1: A model for the *enhancesome* and the mode of HMG box binding to DNA. (A) Structural model of the *enhancesome* derived predominantly from ESI data (*18*, *20*, *21*). The dimerization domain and HMG boxes 1−3 of core UBF are shown as blue ellipsoids and the DNA as a bent red rod. The long arm (N- and C-terminal peptides) of the HMG boxes and the inter box linkers are shown checkered. Linker lengths are approximately to scale, but their indicated positions are purely speculative, the longer box 2−3 linker being placed approximately along the major groove. (B) The positions of the ERK1/2 phosphorylation sites within the HMG boxes 1 and 2 of *Xenopus* UBF are indicated as are the sequences of the sites and the corresponding phosphorylation site mutations used in the present study. (C) The HMG box−DNA binary structure for HMG-D (*38*) is used as a generalized model for nonsequence-specific HMG boxes. The position within this structure corresponding to the ERK phosphorylation site of UBF boxes 1 and 2 is indicated by "PO_4". The incoming and exiting DNA duplexes have been extended by solid red cylinders to better indicate the DNA bend induced by HMG-D. (D) The upper panels show the ERK2 phosphorylation of the HMG boxes 1 and 2 of *Xenopus* UBF and of the corresponding ERK-site T−A mutant boxes. "Stain" refers to the coomassie-stained SDS−PAGE and "PO_4" to the Phosphoimager analysis of these gels. The lower graphic displays the relevant regions of HPLC fractionation of trypsin-digested unphosphorylated and partially phosphorylated HMG box 1. MALDI-TOF was used to identify and to quantitate the peptides in each HPLC fraction, and the data are given as a histogram.

found bound throughout the transcribed region of the ribosomal genes and indeed throughout the whole gene repeat unit (*16*−*18*). Thus, it would appear more likely that UBF defines a specialized ribosomal gene chromatin (rchromatin) and hence might regulate gene activity by modulating accessibility to this chromatin.

UBF bends about 140 bp of ribosomal DNA into a near 360° loop, a structure that is called the ribosomal *enhancesome* and distantly resembles the chromatin nucleosome (*18*−*21*), Figure 1A. This DNA looping is the result of in-phase bending induced by the three N-terminal HMG boxes of UBF, Figure 1A,B (*18*, *21*; see also *6*, *22*). In a recent study, we have found that ribosomal transcription is regulated at the level of the transcription elongation (*23*). Surprisingly, we found that UBF presents a very effective block to the elongating RPI and that ERK phosphorylation of UBF relieved the blockage, allowing unimpeded passage to the polymerase (*23*). Here, we have studied the structural effects of phosphorylating and pseudophosphorylating the ERK sites on UBF. Our findings demonstrate that ERK phosphorylation leads to a major unfolding of the *enhancesome* structure. The data, thus, suggest that RPI transcription is growth-regulated by the remodeling of rchromatin.

EXPERIMENTAL PROCEDURES

Isolation and Expression of Xenopus UBF Mutants. Mutants were assembled in the vector pGEX-2T, expressed in *Escherichia coli* and purified as previously described (*19*, *24*). Nbox123 (core UBF) was produced by fusing amino acids 16−383 of *Xenopus laevis* UBF2b (*25*) to GST, which was not cleaved from the final product. Point mutations were introduced by PCR using mutated primers and were each sequenced. UBF box 1 (amino acids 110−184) and box 2 (amino acids 194−266) as well as the box 1-T117E and

T117A and the box 2-T201E and T201A mutants were expressed in *E. coli* after subcloning from *X. laevis* UBF2 into the *Bam*HI/*Eco*RI site of pGEX2T.

Cruciform DNA Mobility Shift Assays. The cruciform DNA structure was prepared according to procedures in ref *26*. Four oligonucleotides, one of them ^{32}P-end-labeled: 5′-CCCTATAACCCCTGCATTGAATTCCAGTCTGATAA-3′; 5′-GTAGTCGTGATAGGTGCAGGGGTTATAGGG-3′; 5′-AACAGTAGCTCTTATTCGAGCTCGCGCCCTATCAC-GACTA-3; and 5′-TTTATCAGACTGGAATTCAAGCGC-GAGCTCGAATAAGAGCTACTGT-3′ were annealed in TMS (100 mM NaCl, 10 mM Tris-HCl, pH 7.5, and 10 mM $MgCl_2$) and subsequently eluted from a 6.5% PAGE, 1× TBE. Each mobility shift reaction was performed in 10 μL consisting of 5 μL of 2× Binding Buffer (16% Ficoll, 200 mM NaCl, 20 mM HEPES, pH 7.9, 10 mM KCl, 2 mM EDTA, 2 mM spermidine, and 1 mM DTT), 2 μL (100 fmol) of cruciform DNA in TMS (TBS plus 10 mM $MgCl_2$), and 3 μL of TBS (10 mM Tris-HCl, pH7.5, and 100 mM NaCl) containing varying amounts of the respective HMG box proteins. ERK-phosphorylated HMG boxes were added in kinase buffer; see below. After 30 min incubation on ice and the addition of 1 μL of 0.1% xylene cyanol, the samples were loaded on a 6.5% PAGE (30 acrylamide:0.8 bisacrylamide) in 0.5× TBE, separated for 4 h at 11 V/cm, dried, and autoradiographed. In the case of competition assays, complexes on the cruciform DNA were first allowed to assemble for 10 min on ice, then the given excess of linear double-stranded RNA polymerase I promoter UCE DNA (5′-GTTCAGGTGTCCGTGTCGCGCGTCGCCTGGGCCGGC-GGCGCAG) was added, and complexes were incubated for a further 60 min on ice before analysis. This incubation time was determined to allow the reactions to achieve equilibrium binding to the two DNAs. Upshifts used polyclonal antibodies raised against either homogeneous xUBF-HMG box 1 or full-length xUBF.

ERK Phosphorylation of Recombinant HMG1 Boxes in Vitro. The purified HMG boxes 1 and 2 of xUBF were phosphorylated in vitro using MEK1-activated ERK2 (*27*). One nanomole of bacterially expressed HMG box was phosphorylated by activated ERK2 in 30 μL of kinase buffer (20 mM HEPES, pH 7.3, 10 mM $MgCl_2$, 1 mM benzamidine, and 1 mM DTT) containing 1 mM ATP (1 μCi γ[^{32}P]ATP) and incubated at 30 °C for 30 min. Mock phosphorylation was performed either in the absence of ATP or using heat-inactivated ERK2. Microbore HPLC−C_{18} (2−80% CH_3CN, 0.1%TFA) fractions of partially (∼30%) ERK2-phosphorylated, trypsin-digested HMG-box1 were analyzed by MALDI-TOF (Proteomic and Mass Spectrometry Centre, University of Toronto) to identify peptides. Measured masses deviated from those calculated by less than 0.2 Da.

DNase Footprinting. Footprinting was carried out as previously described (*28*). Briefly, unless otherwise indicated, 3 pmol wild-type, mutant, or ERK2-phosphorylated Nbox123 protein was incubated with 3 ng of 5′-[^{32}P]-labeled DNA template (−317 to +118 of the *X. laevis* ribosomal gene) in 50 μL (80 mM KCl, 10% glycerol, 0.1 mM EDTA, 0.5 mM DTT, 10 mM HEPES, pH 7.9, and 0.01 mg/mL poly dA−T) for 15 min on ice. After the addition of 50 μL of DNaseI buffer (10 mM $MgCl_2$ and 5 mM $CaCl_2$) and 5 μL of DNase I, reactions were incubated for 2 min at room temperature and then stopped by the addition of 100 μL of STOP buffer (1% SDS, 0.2 M NaCl, and 20 mM EDTA). Footprints were resolved on 8% TBE−urea sequencing gels and data analyzed on a STORM 860 PhosphorImager (Molecular Dynamics).

ESI Analysis of Protein−DNA Complexes. Core wild-type UBF and T117E and T210E mutants (amino acids 1−370) were expressed and used as GST-fusions as previously described (*18*). Each UBF (1 μg) was incubated in 25 μL of 50 mM HEPES (pH 7.6), 5 mM $MgCl_2$, 80 mM KCl, and 1 mM DTT with 200 ng of the *X. laevis* 1.1 kb *BamHI* enhancer DNA fragment (*29*, *30*). After 15 min at room temperature, the mixture was chromatographed on a 0.5 mL column of Sepharose CL-2B to separate DNA-bound UBF from free protein. The column buffer contained 10 mM HEPES (pH 7.2), 5 mM $MgCl_2$, 1% formaldehyde, and 0.5% glutaraldehyde. The peak DNA fraction (5 μL) was placed on a 1000-mesh copper electron microscope grid, which had been coated with a 3 nm carbon film and glow-discharged immediately before use (*31*). After 30 s, excess sample was washed from the grid with H_2O and the grid was air-dried after all but a thin layer of the H_2O had been removed.

ESI analysis of DNA−protein complexes has been previously described (*31*, *32*). A brief description follows. Estimation of the masses of the UBF−DNA complexes was carried out on a reference image recorded at 120 eV in the electron energy loss spectrum. DNA was used as an internal mass standard, and the mass of the complex was estimated by comparison of integrated optical density of the complex with the integrated optical density over a defined length of DNA. Net phosphorus images were obtained by subtraction of the 120 eV reference image from a 155 eV energy loss image recorded at the peak of the phosphorus L2,3 ionization edge, after alignment and normalization. Results were compared quantitatively with a multiple parameter background correction using two pre-edge images recorded at 105 and 120 eV (see ref *31*).

RESULTS

The nonspecific subclass of HMG boxes, to which those of UBF belong, do not selectively bind DNA, and hence, their binding properties are difficult to analyze by such common techniques as electrophoretic mobility shift analysis (EMSA) or gel shift for short. However, in general, HMG boxes strongly bend the DNA to which they bind (*33*), and the HMG boxes of UBF are no exception to this rule (*18*). Not surprisingly, therefore, HMG boxes display an elevated selectivity for, and binding to, naturally bent or highly flexible DNAs. In particular, HMG boxes typically bind cruciform DNA structures with a K_D of the order of 10^{-6} M (*34*). Thus, we first analyzed the binding of the HMG boxes 1 and 2 of *Xenopus* UBF to cruciform DNA.

Cruciform Binding by the HMG Boxes of UBF Is Only Minimally Affected by Mutation of the ERK Sites. HMG boxes 1 and 2 of xUBF and corresponding ERK site mutant boxes were expressed in bacteria and purified by affinity, Figure 2C. The K_D for binding of the wild-type HMG box 1 of UBF to cruciform DNA was estimated from gel shift assays to be about 1 μM, Figure 2A, and corresponded to that measured previously for the same combination of HMG box and cruciform DNA sequence (*34*). Though HMG box

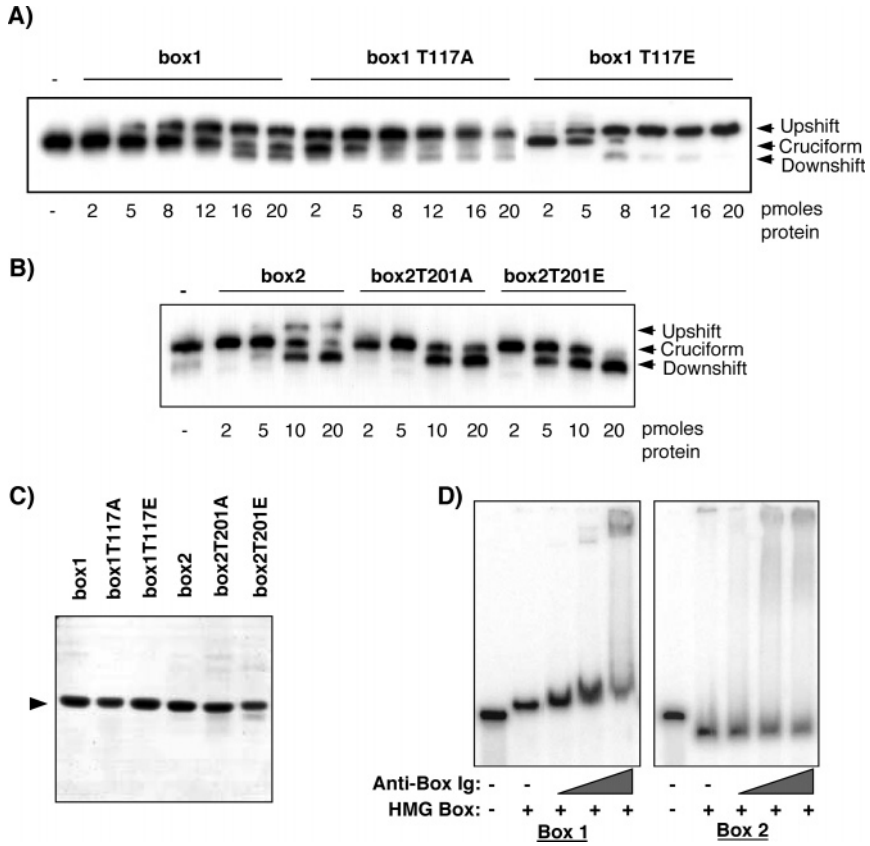

FIGURE 2: The binding of the UBF HMG boxes to cruciform DNA is not significantly affected by the ERK site mutations. Increasing amounts of wild-type and mutant HMG box 1 (A) and box 2 (B) were used in gel shift assays with a 100 fmol of cruciform DNA complex; see Experimental Procedures. (C) Typical SDS−PAGE, coomassie blue-stained analysis of HMG box proteins used in this study. (D) Upshift of HMG box−cruciform complexes with polyclonal anti-xUBF antibodies; left panel, anti-UBF box1; right panel anti-UBF box2.

1 predominantly induced an upshift of the cruciform DNA, some downshifting, that is, toward higher mobility, was also observed. When HMG box 2 was analyzed, the predominant shift was toward higher mobility. Despite this difference, the K_D for cruciform binding by HMG box 2 was about 3 μM, that is, quite similar to box 1 and again well within the typical range for HMG boxes. Both the up- and downshifts observed for boxes 1 and 2 could be further upshifted by antibodies directed against these boxes, demonstrating that the gel shifts were indeed due to binding by the respective HMG boxes, Figure 2D. Cruciform downshifts are probably due to the induction or stabilization of a slightly different cruciform conformation (*34*), but, as will be seen in Figure 4, small amounts of Mg^{2+} eliminated this downshift without affecting the HMG box binding parameters.

Neither the T−A mutation of the ERK site of box 1 nor of box 2 reduced the affinity of these boxes for cruciform DNA, Figure 2. The T−A mutations, therefore, did not significantly affect the structure of either box. Indeed, the T−A mutant box 1 displayed an enhanced affinity for the cruciform DNA, binding 4−5 times more tightly than the wild-type, while the corresponding mutation in box 2 had little or no effect. Our previous observations of DNA bending by these boxes had assigned a large 73° ± 12° bend to box 1 but only a 7° bend to box 2 (*18*). Thus, the increase in affinity of box 1 due to the T−A mutation also corresponded with the preference of this box for a larger DNA bend angle. The N-terminal peptide of the HMG boxes has been shown to lie in a broadened DNA minor groove, Figure 1C. Thus, exchange of the relatively bulky threonine side chain for a single methyl group might then have optimized HMG box contacts with the bent DNA substrate. However, the T−E mutation of HMG box 1 also increased the affinity of this box for cruciform DNA, though to a lesser extent than did the T−A mutation. On the other hand, the T−E mutation of box 2, as the T−A mutation, had no significant effect on cruciform binding by box 2. Thus, while mutation of the ERK sites of box 1, but not of box 2, increased affinity for cruciform DNA, none of the mutations led to a reduction in affinity. This was a somewhat surprising result, given that previous data suggested that phosphorylation of HMG box 1 reduced its binding to linear DNA (*2*).

ERK Site Mutations Affect the HMG Box Affinities for Linear DNA. The very limited effects of the ERK site mutations on the affinity of the HMG boxes for cruciform DNA showed that the structures of the boxes had certainly not been affected by these mutations. We next asked whether the T−E mutations simulated the phosphorylated state of the boxes by significantly reducing their affinity for their natural substrate, the linear ribosomal DNA. To determine this, a natural UBF-preferred site from the UCE of the human RPI promoter (*14*) was used to compete with cruciform DNA for the HMG boxes.

The wild-type HMG box 1 and 2 complexes on cruciform DNA were partially competed by a 10−50-fold excess of linear UCE duplex DNA and fully competed by a 100-fold

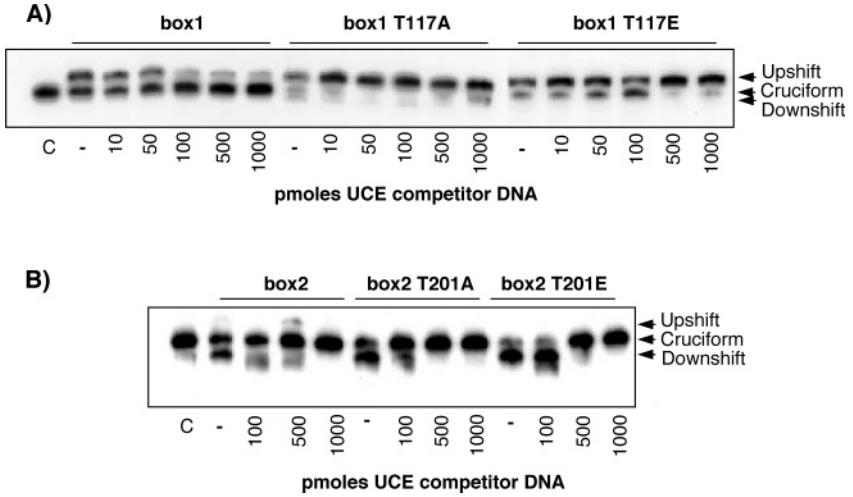

FIGURE 3: ERK site mutant boxes have a reduced affinity for linear duplex DNA. Wild-type and mutant HMG box 1 (A) and box 2 (B) (10 pmol) complexed with cruciform DNA (100 fmol) were subjected to a challenge with increasing amounts of a linear duplex UCE DNA. In both cases, the T−E mutation reduced the affinity for the linear DNA; see Experimental Procedures.

excess, Figure 3. Thus, the K_d values of both boxes for the linear DNA duplex lay between 10^{-4} and 10^{-5} M, similar to that estimated previously for box 1 and for other sequence nonspecific HMG boxes (*19*, *33*). The linear UCE DNA was, however, unable to detectably compete for the mutant box 1, Figure 3A. The T−E mutant box 1 formed cruciform complexes, which were completely resistant to competition even by a 1000-fold excess of UCE DNA. Surprisingly, T−A mutation of box 1 had a very similar effect, also reducing the K_d for the linear UCE DNA to well below 10^{-3} M. However, when HMG box 2 was similarly analyzed, only the T−E mutation reduced its affinity for the linear DNA. The T−E mutant box 2−cruciform complex could not be competed by a 100-fold excess of UCE DNA, but was fully competed by a 500-fold excess. Thus, T−E mutation of HMG box 2 caused a 10 times reduction in affinity for the linear UCE DNA, that is, to between 10^{-3} and 10^{-4} M.

The T−E mutation of the ERK sites of both HMG boxes 1 and 2 significantly reduced their affinity for the linear ribosomal DNA, but in the context of HMG box 2, the T−E mutation had a significantly smaller effect than in the context of box 1. Quite unexpectedly, the T−A mutation also severely reduced the affinity of box 1, but not of box 2, for linear DNA. Though we presently have no structural explanation for this effect, it does underline the key role the N-terminal peptide plays in DNA binding by the HMG boxes (*33*). The much greater DNA bend angle ascribed to HMG box 1 (*18*) clearly correlated with the more severe effects of the ERK site mutations, suggesting that these mutations specifically affect the ability of this box to bend DNA.

Phosphorylation of HMG Boxes 1 and 2 Reduces Binding to Linear but Not Cruciform DNA. When a coupled MEK-ERK expression system was used (*27*), HMG boxes 1 and 2 of UBF were also stoichiometrically phosphorylated and assayed for cruciform and linear DNA binding, see Experimental Procedures. The specificity of the ERK2 phosphorylation was previously described (*2*) but was verified here for each of the boxes, Figure 1D. Phosphorylation was fully blocked by mutation of the ERK sites. Further, MALDI-TOF analysis of tryptic digests of box 1 directly identified the phosphorylated peptide. Considering the bulk of the phosphate group, we were very surprised to find that the boxes bound cruciform DNA with an affinity similar if not identical with that of the unphosphorylated boxes, Figure 4A,C. (Upshifts were systematically observed in these experiments. This was found to be due to the addition of the HMG boxes in kinase buffer, the resulting final 3 mM $MgCl_2$ concentration changing the conformational preference of the cruciform.) However, while the unphosphorylated HMG box/cruciform complexes could be competed with linear UCE DNA, this was not the case for the phosphorylated boxes, Figure 4B,D. Affinity for linear DNA was reduced by at least 4 times for box 1 and at least 2 times for box 2. Thus, the phospho-boxes behaved as did their corresponding ERK site T−E mutants, confirming that these mutations closely simulated HMG box phosphorylation.

Phosphorylation of Core UBF Changes Its Mode but Not Its Affinity of DNA Binding. Since T−E mutation of HMG boxes 1 and 2 closely simulated their phosphorylation, we used these mutations to determine if UBF phosphorylation affected the architecture of ribosomal DNA within the *enhancesome*. As described above, the *enhancesome* is formed when a dimer of UBF binds around 140 bp of ribosomal DNA, and its formation requires only the core of UBF, that is, the N-terminal dimerization domain and HMG boxes 1−3 of UBF (Nbox123); see Figure 1A,B. We first DNaseI-footprinted single and double ERK site mutants of core UBF (Nbox123) on the *Xenopus* RPI promoter, Figure 5; see Experimental Procedures. Consistent with the known binding mode of core UBF (*19*), mutation of HMG box 1 (Nbox123-T117E) affected the DNA hypersensitivity immediately flanking the binding site of this box at −22, +1, and +22, whereas mutation of the site in HMG box 2 (Nbox123-T201E) did not display these effects. The double mutant T117/201E essentially eliminated all DNase I hypersensitivity due to Nbox123 binding. Surprisingly, none of the Nbox123 mutations, including the T117/201E double mutation, significantly affected overall protection of the DNA. Titration of DNA accessibility at the initiation site, using the protection/hypersensitivities of bases −2 to +1, Figure 5, revealed that the affinity of wild-type Nbox123

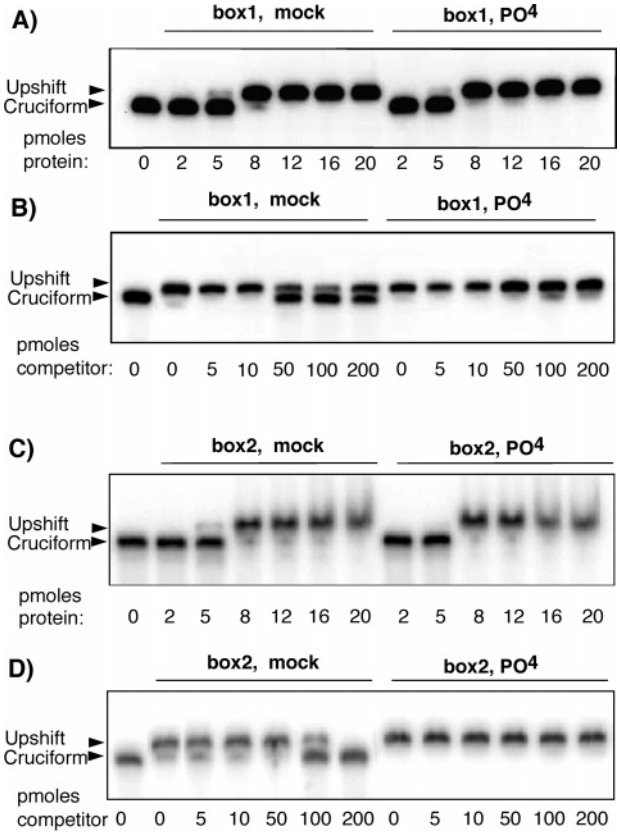

FIGURE 4: Phosphorylated HMG boxes 1 and 2 bind cruciform DNA normally, but have reduced affinity for linear DNA. Wild-type HMG boxes 1 and 2 were phosphorylated "PO_4" or mock-phosphorylated "mock" in vitro with activated ERK; see Experimental Procedures. (A and C)Gel shift assays with increasing amounts of phosphorylated (A) and mock-treated (C) wild-type HMG box 1 and box 2, respectively, with 100 fmol cruciform DNA. (B and D) Phosphorylated and mock-treated wild-type HMG box 1 and box 2, respectively (10 pmol), complexed with cruciform DNA (100 fmol) were subjected to a challenge with increasing amounts of a linear duplex UCE DNA.

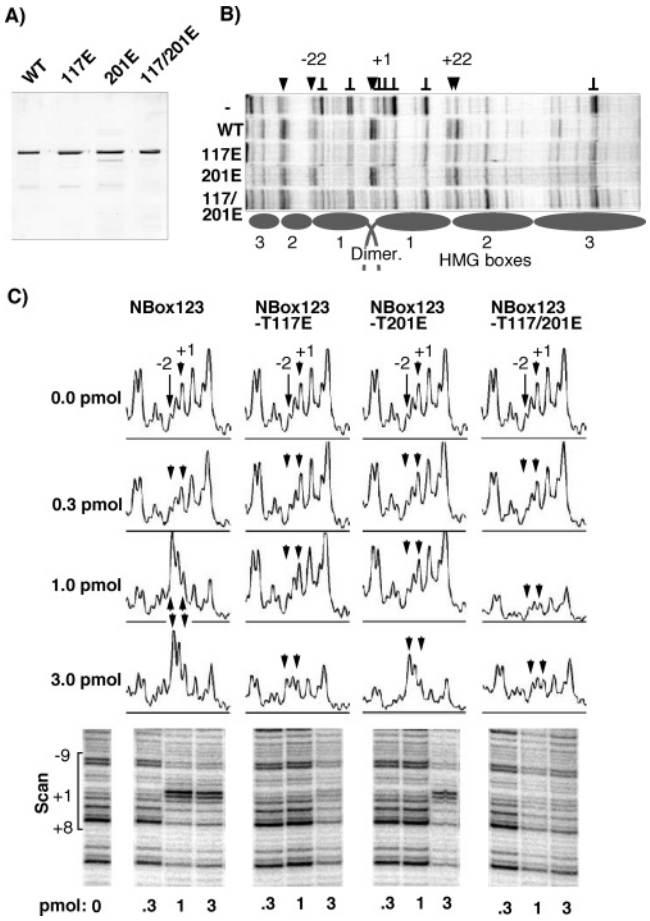

FIGURE 5: Pseudophosphorylation of core UBF affects its ability to induce DNaseI hypersensitivity in the RPI promoter but does not affect its ability to protect the DNA nor its DNA affinity. (A) Coomassie-stained SDS−PAGE analysis of the Nbox123 proteins. (B) Footprints of the wild-type (wt) and each of the Nbox123 mutants as compared with the naked DNA. Nbox123 hypersensitive sites are indicated by arrowheads and protection by "⊥". (C) Quantitative footprinting of the wt and mutant Nbox123 proteins. Three amounts of Nbox123 proteins were analyzed, 0.3, 1, and 3 pmol. Base positions relative to the initiation site at +1 are indicated, and the initiation site regions density scans are shown for the gel region indicated (Scans).

and the T117/201E ERK site mutant were indistinguishable, close to the previously determined K_d of 20×10^{-9}M (*19*), while the single site mutants displayed a slightly reduced affinity.

As with the T−E mutations, ERK phosphorylation did not significantly affect the overall binding affinity of Nbox123, but did drastically change the observed pattern of DNA hypersensitivity, Figure 6. The Nbox123-T201E mutant was used in these experiments to achieve the near-stoichiometric phosphorylation of HMG box 1 necessary to observe footprinting changes. ERK phosphorylation essentially eliminated the +2 and all other hypersensitive sites associated with HMG box 1 binding and bending, but did not affect overall pattern of protection.

Simulated Phosphorylation of the ERK Sites Prevents Enhancesome Formation. Visualization of complexes formed between T117E (box 1) and T201E (box 2) mutant core UBF and the ribosomal DNA by electron spectroscopic imaging (ESI) revealed that neither form of UBF was able to induce the 360° DNA looping characteristic of the *enhancesome*; in Figure 7, compare examples in panels B and C with panel A. The ESI technique allows the quantitation of both the protein and DNA composition of individual complexes. A majority (60%) of complexes contained a UBF dimer (137 ± 14 kDa, core UBF dimer has an M_r of 147 kDa), Figure 7D,E. However, 85% of the complexes contained half the DNA than normally found in the *enhancesome* (58 ± 35 bp versus the expected 135 bp). The folding of DNA within the mutant complexes was also quite unlike that seen in the unmodified *enhancesome*; in Figure 7, compare images B and C with A. DNA within the mutant complexes showed no sign of a 360° loop and was unusually compacted and appeared to be tightly kinked. Thus, even though a dimer of UBF was present in these complexes, at most only three HMG boxes could effectively contact the DNA, leaving half the enhancesome DNA free. A somewhat similar situation had previously been observed when UBF dimerization was prevented (*18*). However, in that case, the DNA was clearly bent into a half enhancesomal turn, quite unlike the complexes observed here. Thus, the ERK site mutations not only prevented the interaction of core UBF with a full 135 bp of *enhancesomal* DNA but also drastically altered the conformation of this DNA, preventing the normal in-phase bending necessary to form the *enhancesome*.

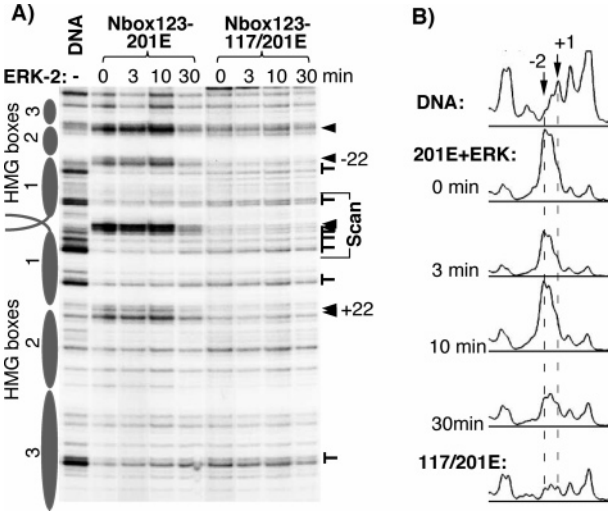

FIGURE 6: Increasing levels of ERK phosphorylation of HMG box 1 of core UBF prevent the DNase I hypersensitivity induced by this box but not the protection of the rDNA. (A) DNase I footprinting of 3 pmol of the single Nbox123-T201E and double -T117/201E HMG box mutants after increasing ERK2 phosphorylation as compared with naked DNA (DNA). Nbox123 hypersensitive sites are indicated by arrowheads and protection by "⊥". (B) Density profile of panel A over the RPI initiation site region, "Scan" in panel A.

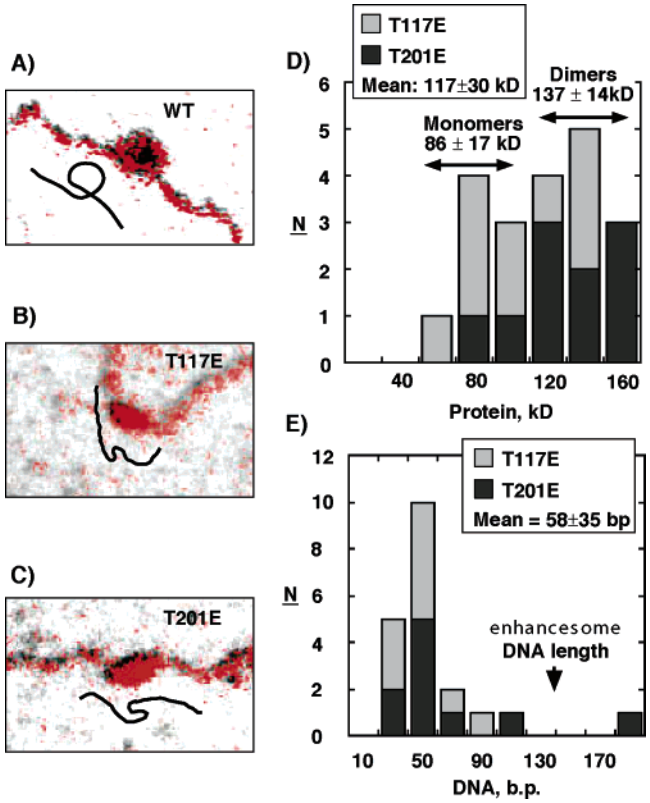

FIGURE 7: Formation of the *enhancesome* is prevented by UBF mutations that simulate ERK phosphorylation. (A−C) Examples of UBF−DNA complexes formed with wild-type core UBF and the core UBF-T117E and T201E mutants. The total mass image, in gray tone, is shown overlayed by the false color net phosphorus (DNA) image in red. The DNA image has been slightly displaced toward the bottom right to aid visibility. The probable DNA trajectories through the complexes are indicated by a line diagram in black. In the case of panels B and C, these trajectories are no more than conjecture due to compaction of the DNA component. (D and E) The masses of both protein and DNA components of the mutant complexes. The measured protein and DNA masses of all T117E and T210E−UBF complexes analyzed are given in histogram form. The data have been "binned" into 20 kDa or 20 bp intervals, but the mean and standard deviations were calculated directly from the "unbinned" data. The expected UBF protein monomer and dimer masses are indicated as is the DNA content of the enhancesome (*18*).

DISCUSSION

Our data demonstrate that phosphorylation of the MAP-kinase (ERK) sites in HMG boxes 1 and 2 of UBF very significantly changes their interaction with linear but not bent DNA, leading to extensive changes in the structure of the *enhancesome*. Phosphorylation of UBF by ERK is a necessary step in the activation of ribosomal transcription by growth factors such as EGF (*2*). Our data, therefore, show that activation of the ERK signaling cascade more than likely regulates ribosomal transcription by modulating ribosomal DNA folding and its interactions with UBF. The data may also provide the basis for a structural explanation as to why the ERK site mutant UBFs are unable to mediate activation of ribosomal gene transcription (*2*).

The molecular basis for the architectural changes induced by ERK phosphorylation of UBF can be deduced from the effects ERK phosphorylation and pseudophosphorylation (T−E mutation) of the HMG boxes have on their DNA binding properties. We previously showed that ERK phosphorylation partially abrogates the interaction of the UBF HMG box 1 with a linear target DNA (*2*). The present data show that pseudophosphorylation of both HMG boxes 1 and 2 significantly reduced their affinities for linear target DNA. However, these same mutations had little or no effect on binding to cruciform ("bent") DNA. The same was true for the stoichiometrically phosphorylated HMG boxes of UBF. The data suggest that ERK site phosphorylation and ERK site mutation act in a very similar way, not so much to prevent DNA binding as to reduce the capacity of the boxes to bend DNA. This was confirmed when the DNA affinity of mutant core UBF and the low-resolution structures of mutant *enhancesomes* were determined. Complexes formed between pseudophosphorylated core UBF, and linear ribosomal DNA displayed a loss of DNaseI hypersensitivity, but little or no change in DNA binding constant was detected. The complexes predominantly contained the expected dimer of core UBF, associated with only half the *enhancesomal* DNA. Further, the DNA that remained closely associated with the mutant complex, though compacted, no longer displayed the 360° coiling characteristic of the *enhancesome*. The inability to coil DNA was clearly consistent with the conclusion that the individual mutant HMG boxes were unable to bend DNA. The fact that mutant complexes contained only half the normal *enhancesome* DNA may also be indicative of a change in the bending capacity of the HMG boxes; see below.

ESI studies have strongly suggested that the DNA architecture of the *enhancesome* results from six in-phase bends induced by six HMG boxes of a dimer of UBF, Figure 1A (*18*, *21*). For each of these bends to be in-phase, the relative position of HMG box binding must be precisely defined. Each HMG box of UBF is tethered to the previous box by a conserved inter-box peptide. In the case of boxes 1 and 2, this peptide is so short that it is necessary to postulate these boxes sit head-to-head along the DNA (*21*); see

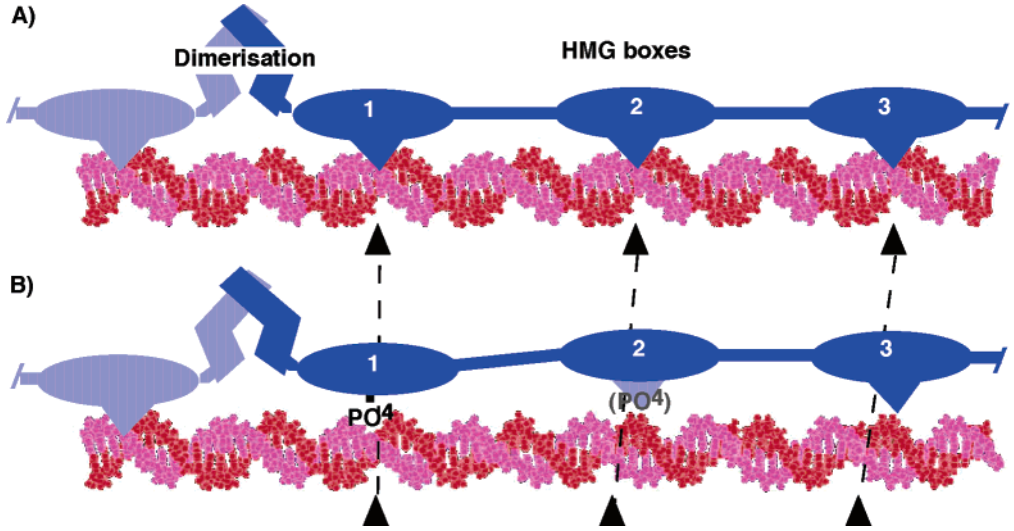

FIGURE 8: Diagrammatic representation of the possible effects of HMG box phosphorylation on the capacity of the adjacent HMG boxes to bind to DNA. The HMG boxes are shown as blue ellipsoids joined by rigid linker peptides. (A) When the HMG boxes are not phosphorylated, the minor groove binding sites for adjacent HMG boxes lie aligned along the upper surface of the DNA (red/purple). (B) When the N-terminal and/or second HMG box is phosphorylated, it is loosened from the DNA. The resulting loss of bending and unwinding of the DNA helix decreases its pitch displacing the minor groove binding sites, making them inaccessible to the subsequent boxes. A large segment of the DNA is, thus, cooperatively released from UBF.

chequered domains in Figure 1A. This, and the fact that UBF can induce the same *enhancesomal* DNA looping on almost any DNA sequence, even bacterial (*18*), strongly suggests that the positioning of the HMG boxes along the DNA, and hence the position of in-phase bends, is strictly controlled by the inter-box peptides; see Figure 8. Thus, if one HMG box were prevented from bending DNA, the resulting local change in DNA pitch would displace the minor groove sites of the adjacent HMG boxes around the DNA surface, preventing these boxes from binding the DNA in the minor groove. This would lead to a cooperative release of a large segment of the *enhancesomal* DNA, such as the one we have observed. The unphosphorylated (unmutated) HMG boxes, freed in this way, might still fold back to find other, imperfect DNA sites within easy reach, leading to the compaction that we observed by ESI.

Our data demonstrate that phosphorylation of UBF by the MAP-kinase cascade leads to very significant changes in DNA architecture within the *enhancesome*. Our earlier suggestion that the *enhancesome* represents the primary unit of a specialized ribosomal chromatin (*35*, *36*) has now been validated. ChIP assays have demonstrated that UBF binds throughout the ribosomal gene repeat, even within its transcribed regions (*16*). Thus, the transcribing polymerase is necessarily faced with negotiating a passage through an *enhancesome* array in vivo. We have recently shown that RPI transcription is regulated at the level of elongation and that UBF phosphorylation by ERK facilitates the passage of the polymerase through *enhancesomal* DNA (*23*). The present data suggest that this is achieved by transiently releasing short segments of DNA from UBF, a mechanism analogous to the opening/remodeling of nucleosomal chromatin. It has been shown that UBF can interact, though weakly, with nucleosomes (*36*, *37*), and the *enhancesome* could logically harbor the octamer of core histones (*18*). It is now important to deduce whether the *enhancesome* and the nucleosome are exclusive structures in vivo, and if not, how they might coexist.

ACKNOWLEDGMENT

We would like to thank Dr. M. Cobb for allowing us to use the ERK-MEK coupled expression system and Dr. C. Chrestensen for supplying us the vector and much useful guidance and advice on its use. We also thank Dr. R. Reeder for the anti-xUBF antibody. This work was supported by an operating grant from the Canadian Institutes of Health Research and a FCAR-FRSQ Santé (Québec) scholarship to G.P.

REFERENCES

1. Liebhaber, S. A., Wolf, S., and Schlessinger, D. (1978) Differences in rRNA metabolism of primary and SV40-transformed human fibroblasts, *Cell 13*, 121−127.
2. Stefanovsky, V. Y., Pelletier, G., Hannan, R., Gagnon-Kugler, T., Rothblum, L. I., and Moss, T. (2001) An immediate response of ribosomal transcription to growth factor stimulation in mammals is mediated by ERK phosphorylation of UBF, *Mol. Cell 8*, 1063−1073.
3. Lewis, J. D., and Tollervey, D. (2000) Like attracts like: getting RNA processing together in the nucleus, *Science 288*, 1385−1389.
4. Dundr, M., and Misteli, T. (2001) Functional architecture in the cell nucleus, *Biochem. J. 356*, 297−310.
5. Visintin, R., and Amon, A. (2000) The nucleolus: the magician's hat for cell cycle tricks, *Curr. Opin. Cell Biol. 12*, 372−377.
6. Moss, T. (2004) At the crossroads of growth control; making ribosomal RNA, *Curr. Opin. Genet. Dev. 14*, 210−217.
7. Olson, M. O. (2004) Sensing cellular stress: another new function for the nucleolus?, *Sci. STKE 2004*, pe10.
8. Zhao, J., Yuan, X., Frodin, M., and Grummt, I. (2003) ERK-dependent phosphorylation of the transcription initiation factor TIF-IA is required for RNA polymerase I transcription and cell growth, *Mol. Cell 11*, 405−413.
9. Bell, S. P., Learned, R. M., Jantzen, H. M., and Tjian, R. (1988) Functional cooperativity between transcription factors UBF1 and SL1 mediates human ribosomal RNA synthesis, *Science 241*, 1192−1197.
10. Pikaard, C. S., McStay, B., Schultz, M. C., Bell, S. P., and Reeder, R. H. (1989) The Xenopus ribosomal gene enhancers bind an essential polymerase I transcription factor, xUBF, *Genes Dev. 3*, 1779−1788.
11. Smith, S. D., Oriahi, E., Lowe, D., Yang-Yen, H.-F., O'Mahony, D., Rose, K., Chen, K., and Rothblum, L. I. (1990) Characteriza-

tion of factors that direct transcription of rat ribosomal DNA, *Mol. Cell. Biol. 10*, 3105−3116.
12. McStay, B., Frazier, M. W., and Reeder, R. H. (1991) xUBF contains a novel dimerization domain essential for RNA polymerase I transcription, *Genes Dev. 5*, 1957−1968.
13. Schnapp, A., and Grummt, I. (1991) Transcription complex formation at the mouse rDNA promoter involves the stepwise association of four transcription factors and RNA polymerase I, *J. Biol. Chem. 266*, 24588−24595.
14. Jantzen, H. M., Chow, A. M., King, D. S., and Tjian, R. (1992) Multiple domains of the RNA polymerase I activator hUBF interact with the TATA-binding protein complex hSL1 to mediate transcription, *Genes Dev. 6*, 1950−1963.
15. Friedrich, J. K., Panov, K. I., Cabart, P., Russell, J., and Zomerdijk, J. C. (2005) TBP-TAF complex SL1 directs RNA polymerase l PIC formation and stabilises UBF at the rDNA promoter, *J. Biol. Chem*.
16. O'Sullivan, A. C., Sullivan, G. J., and McStay, B. (2002) UBF binding in vivo is not restricted to regulatory sequences within the vertebrate ribosomal DNA repeat, *Mol. Cell. Biol. 22*, 657−668.
17. Copenhaver, G. P., Putnam, C. D., Denton, M. L., and Pikaard, C. S. (1994) The RNA polymerase I transcription factor UBF is a sequence-tolerant HMG-box protein that can recognize structured nucleic acids, *Nucleic Acids Res. 22*, 2651−2657.
18. Stefanovsky, V. Y., Bazett-Jones, D. P., Pelletier, G., and Moss, T. (1996) The DNA supercoiling architecture induced by the transcription factor xUBF requires three of its five HMG-boxes, *Nucleic Acids Res. 24*, 3208−3215.
19. Leblanc, B., Read, C., and Moss, T. (1993) Recognition of the Xenopus ribosomal core promoter by the transcription factor xUBF involves multiple HMG box domains and leads to an xUBF interdomain interaction, *EMBO J. 12*, 513−525.
20. Bazett-Jones, D. P., Leblanc, B., Herfort, M., and Moss, T. (1994) Short-range DNA looping by the Xenopus HMG-box transcription factor, xUBF, *Science 264*, 1134−1137.
21. Stefanovsky, V. Y., Pelletier, G., Bazett-Jones, D. P., Crane-Robinson, C., and Moss, T. (2001) DNA looping in the RNA polymerase I enhancesome is the result of non-cooperative in-phase bending by two UBF molecules, *Nucleic Acids Res. 29*, 3241−3247.
22. Moss, T., and Stefanovsky, V. Y. (2002) At the center of eukaryotic life, *Cell 109*, 545−548.
23. Stefanovsky, V. Y., Langlois, F., Gagnon-Kugler, T., Rothblum, L., and Moss, T. (2006) Growth factor signaling regulates elongation of RNA polymerase I transcription in mammals, a role for UBF phosphorylation and r-chromatin remodeling, *Mol. Cell 21*, in press.
24. Smith, D. B., and Corcoran, L. M. (1991) Protein expression, in *Current Protocols in Molecular Biology* (Ausubel, F. M., Brent, R., Kingston, R. E., Moore, D. D., Seidman, J. G., Smith, J. A., and Struhl, K., Eds.) Greene Publishing Associates & Wiley-Interscience, New York.
25. Bachvarov, D., and Moss, T. (1991) The RNA polymerase I transcription factor xUBF contains 5 tandemly repeated HMG homology boxes, *Nucleic Acids Res. 19*, 2331−2335.
26. Bianchi, M. E. (1988) Interaction of a protein from rat liver nuclei with cruciform DNA, *EMBO J. 7*, 843−849.
27. Wilsbacher, J. L., and Cobb, M. H. (2001) Bacterial expression of activated mitogen-activated protein kinases, *Methods Enzymol. 332*, 387−400.
28. Read, C., Larose, A. M., Leblanc, B., Bannister, A. J., Firek, S., Smith, D. R., and Moss, T. (1992) High-resolution studies of the *Xenopus laevis* ribosomal gene promoter in vivo and in vitro, *J. Biol. Chem. 267*, 10961−10967.
29. Moss, T., Boseley, P. G., and Birnstiel, M. L. (1980) More ribosomal spacer sequences from *Xenopus laevis*, *Nucleic Acids Res. 8*, 467−485.
30. De Winter, R. F. J., and Moss, T. (1987) A complex array of sequences enhances ribosomal transcription in *Xenopus laevis*, *J. Mol. Biol. 196*, 813−827.
31. Bazett-Jones, D. P. (1993) Empirical basis for phosphorous mapping and structure determination of DNA:protein complexes by electron spectroscopic imaging, *Microbeam Anal. 2*, 69−79.
32. Bazett-Jones, D. P., and Brown, M. L. (1988) Electron microscopy shows that TFIIIA bends DNA, *Mol. Cell. Biol. 9*, 336−341.
33. Read, C. M., Cary, P. D., Crane-Robinson, C., Driscoll, P. C., Carrillo, M. O. M., and Norman, D. G. (1995) The structure of the HMG box and its interaction with DNA, in *Nucleic Acids and Molecular Biology* (Eckstein, F., and Lilley, D. M. J., Eds.) Vol. 9, pp 222−250, Springer-Verlag, Berlin, Heidelberg, Germany.
34. Pöhler, J. R. G., Norman, D. G., Bramham, J., Bianchi, M. E., and Lilley, D. M. J. (1998) HMG box proteins bind to four-way DNA junctions in their open conformation, *EMBO J. 17*, 817−826.
35. Moss, T., and Stefanovsky, V. Y. (1995) Promotion and regulation of ribosomal transcription in eukaryotes by RNA polymerase I, in *Progress in Nucleic Acids and Molecular Biology* (Cohn, W. E., and Moldave, K., Eds.), pp 25−66, Academic Press, Inc., San Diego, CA.
36. Moss, T., Stefanovsky, V. Y., and Pelletier, G. (1998) The structural and architectural role of upstream binding factor, UBF, in *Transcription of Ribosomal Genes by Eukaryotic RNA Polymerase I* (Paule, M. R., Ed.), pp 75−94, Landes Bioscience, Austin, TX.
37. Kermekchiev, M., Workman, J. L., and Pikaard, C. S. (1997) Nucleosome binding by the polymerase I transactivator upstream binding factor displaces linker histone H1, *Mol. Cell. Biol.*
38. Murphy, F. V., Sweet, R. M., and Churchill, M. E. (1999) The structure of a chromosomal high mobility group protein-DNA complex reveals sequence-neutral mechanisms important for non-sequence-specific DNA recognition, *EMBO J. 18*, 6610−6618.

BI051782H